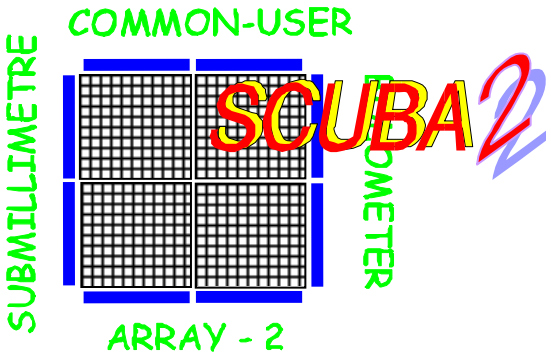

SCUBA-2 FTS Project Office
University of Lethbridge
Physics Department
4401 University Drive
Lethbridge, Alberta
CANADA
T1K 3M4

Tel: 1-403-329-2771
Fax: 1-403-329-2057
Email: brad.gom@uleth.ca
WWW: http://research.uleth.ca/scuba2/

Document Title: FTS-2 Optical Design

Document Number: SC2/FTS/OPT/001

Issue: Version 2.1

Date: 6 November 2006

Document Prepared By:	B. G. Gom FTS-2 Project Manager	Signature and Date:	Brad Gom	06/11/06
Document Approved By:	D. A. Naylor FTS-2 Project Lead	Signature and Date:	David A Naylor	06/11/06
Document Released By:	J. Molnar Canadian Project Manager	Signature and Date:		06/11/06

Change Record

Issue	Date	Section(s) Affected	Description of Change / Change Request Reference / Remarks
0.1	17/05/05	All	First draft
1.0	23/06/05	All	PDR version
2.0	4/11/06	All	CDR version
2.1	6/11/06	5	Added field points

Contents

Applicable and Referenced Documents

Document Number	*Title*	*Version*
INO 060140 R/09	INO Optical Modelling Report	9
SC2/FTS/OPT/004	FTS-2 Optical Prescription	1.0
SC2/FTS/OPT/002	FTS-2 Port Optical Coordinates	1.0
SC2/FTS/OPT/003	FTS-2 Input Port Rotation	1.0
SC2/FTS/MEC/002	FTS-2 Mirror Mount Tests	1.0

1. Introduction

Prof. Naylor has been designing and building Fourier transform spectrometers (FTS) for astronomical and aeronomical use for over 30 years. In the last decade his group has used a variety of FTSs at the JCMT and, during this time, compiled a wealth of knowledge in their use at this telescope. The development of detector systems from single pixel systems to imaging camera arrays has been matched by an evolution in FTS design from the classical Michelson interferometer to the Mach-Zehnder design[1]. As one of the co-developers of the Mach-Zehnder (MZ) concept Prof. Naylor's group has designed, built and operated an MZ FTS at the JCMT[2]. Moreover, his group is the lead institution for Canada's participation in the ESA Herschel/SPIRE project[3], which also involves an MZ FTS[4].

2. Design Constraints

Since the JCMT optical and structural framework designs were fixed before the FTS-2 project began, the FTS-2 optical and mechanical designs are highly interdependent and tightly constrained. FTS-2 intercepts the SCUBA-2 optical beam near an intermediate image surface directly outside the telescope elevation bearing opening (see Figure 1). However, as an ancillary instrument, FTS-2 must not interfere with the SCUBA-2 beam when the FTS is not in use. The telescope dish and receiver cabin access walkway define the horizontal limits of the space envelope for FTS-2. These mechanical constraints were defined from measurements of the backing structure in late March 2005, and with subsequent follow up measurements from Thomas Chylek (JAC) in April.

Within the interferometer, there are additional design constraints that the beams at the rooftop mirrors must be collimated, there must be pupils located at the rooftop mirrors (at the ZPD location) for symmetry, and the beam waist near the beamsplitters must be minimized in order to reduce the beamsplitter diameters. Design goals for the spectrometer included placing both input ports on the sky, placing both output ports on adjacent detector subarrays, maximizing the useable field of view, and providing variable spectral resolution from 0.1 to 0.006 cm^{-1}.

The optical design problem for FTS-2 is essentially to reproduce the original image and pupil at the outputs of the interferometer, while maintaining unity image magnification, in order to allow the instrument to be placed midway through the existing SCUBA-2 feed optics. The optical design is complicated by the limited available space, the curved image surface at the input, and the ~f/7 input beam. It is impossible to achieve diffraction limited imaging at high spectral resolution over the entire SCUBA-2 field of view. Optimizing the resulting trade-off between FOV and spectral resolution within the constraints imposed by the fixed space envelope was a significant challenge.

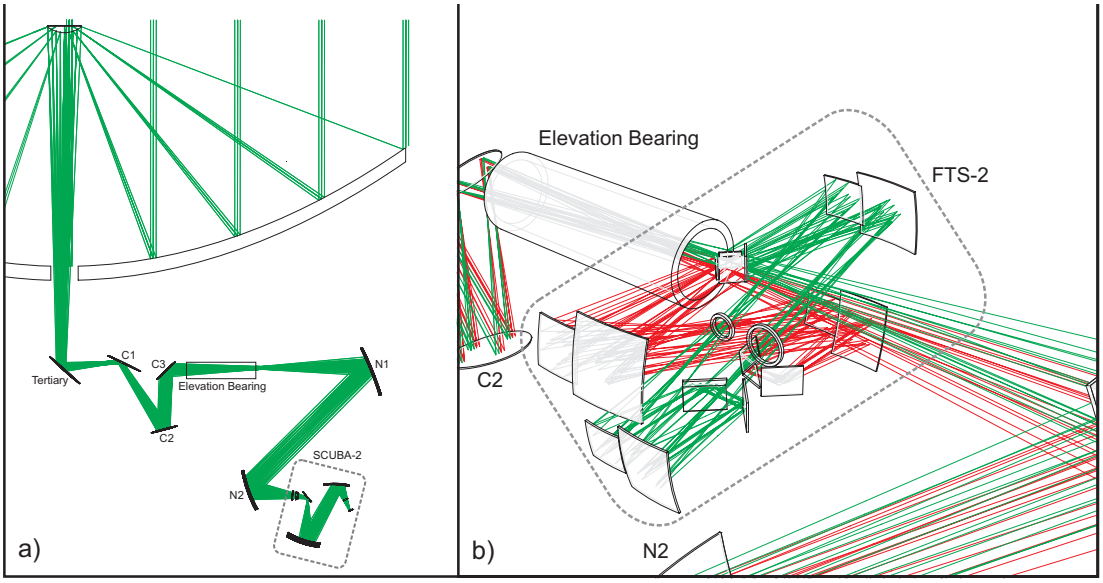

Figure 1. a) A schematic of the SCUBA-2/JCMT optical system, showing the available space for FTS-2 between the elevation bearing and mirror N1. b) The FTS-2 optics at the mounting location.

3. Interferometer Design

The design of FTS-2 is based on the MZ design successfully used at the JCMT for the last four years and is similar to the SPIRE FTS. Unlike the Martin-Puplett interferometer, the MZ design has the advantage of being insensitive to polarization, while providing high and uniform efficiency over a broad wavelength range. The design also provides access to the two input and two output ports of the interferometer. Following a recommendation at the FTS-2 CoDR, the two input ports have been reconfigured to view adjacent regions of the sky providing a differential measurement, which will reduce the effects of varying atmospheric emission during the interferogram acquisition. Similarly, the two output ports have been reconfigured to be directed to two diagonally opposed subarrays of the SCUBA-2 camera. The complementary interferogram signals at these two outputs can, in principle, be recombined to remove post detection common-mode noise, which leads to an increased signal-to-noise ratio of $\sqrt{2}$. Whether this gain can be realized in practice will depend in large measure on the similarities between the arrays, but the design now allows for it. Following a recommendation at the FTS-2 PDR, an ambient load in the form of a simple shutter will be included in one arm of the interferometer, enabling the system to be operated in single input port mode if required.

A simplified optical schematic of FTS-2 is shown in Figure 2. Retractable pickoff mirrors PO1 and PO2 intercept two ~2 arcminute diameter beams from the SCUBA-2 beam as it exits the left telescope elevation bearing tube. The beams are redirected by mirrors FM2_1 and FM2_3 to the first intensity beam divider, BS1. As the moving mirror assembly (consisting of two corner cube retroreflectors, mounted back-to-back on a linear stage) is moved a distance x, an optical path difference of 4x is introduced between the two interferometer arms. The beams are recombined at beam divider BS2, and the two output ports are returned to the SCUBA-2 optical system by mirrors PO2 and PO4.

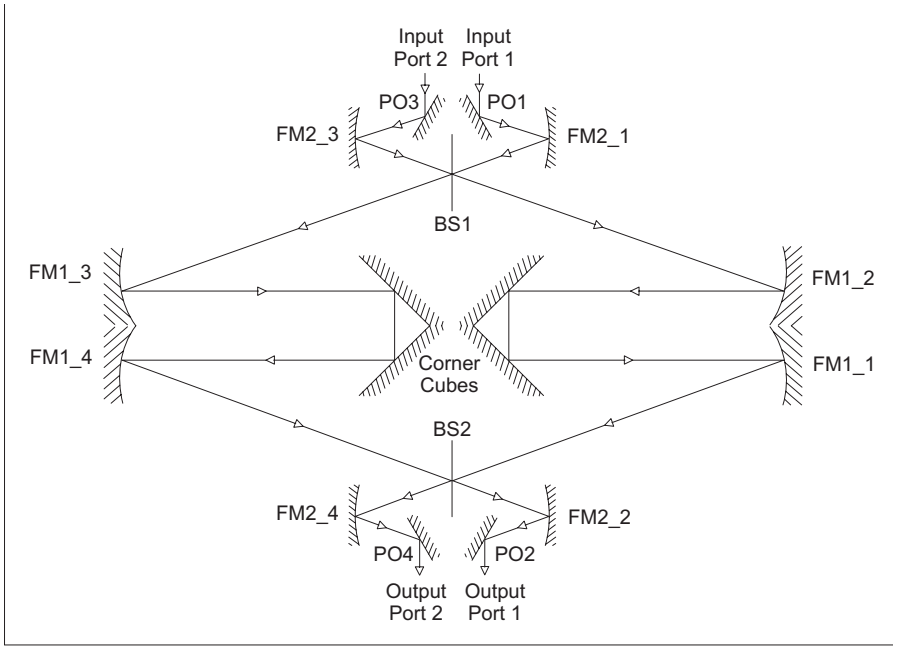

Figure 2. A schematic of the dual-port Mach-Zehnder FTS design.

As mentioned above, the FTS-2 design is based upon that of the SPIRE instrument[3] of ESA's Herschel mission. Following the design of SPIRE powered mirrors within the interferometer will be used to minimize the effects of beam spread. The symmetry of this design minimizes aberrations in the system. The pupils will be placed near the apex of the corner cubes when the stage is near zero path difference (ZPD) position in order to maintain symmetry in the system. The positional accuracy of the Aerotech translation stage with the precision Heidenhain non-contact linear encoder (< 1 μm), and alignment accuracy of the corner cube mirrors (<10 seconds) amply meet the wavefront error requirement derived from modulation efficiency considerations at these long wavelengths. Corner cubes placed back-to-back with coincident apices eliminate tilt, and any shear introduced by the translation stage, but more importantly, provide proper parity of the reflections in the vertically folded design.

The interferometer will be assembled on a damped optical breadboard, with optical components housed in high-precision adjustable mounts. Mirrors will be made from uncoated, diamond turned aluminium, which will allow for alignment at optical wavelengths.

4. Optical Layout

In order to fit in the available space, the interferometer arms are folded vertically as shown in Figure 1a) and Figure 3.

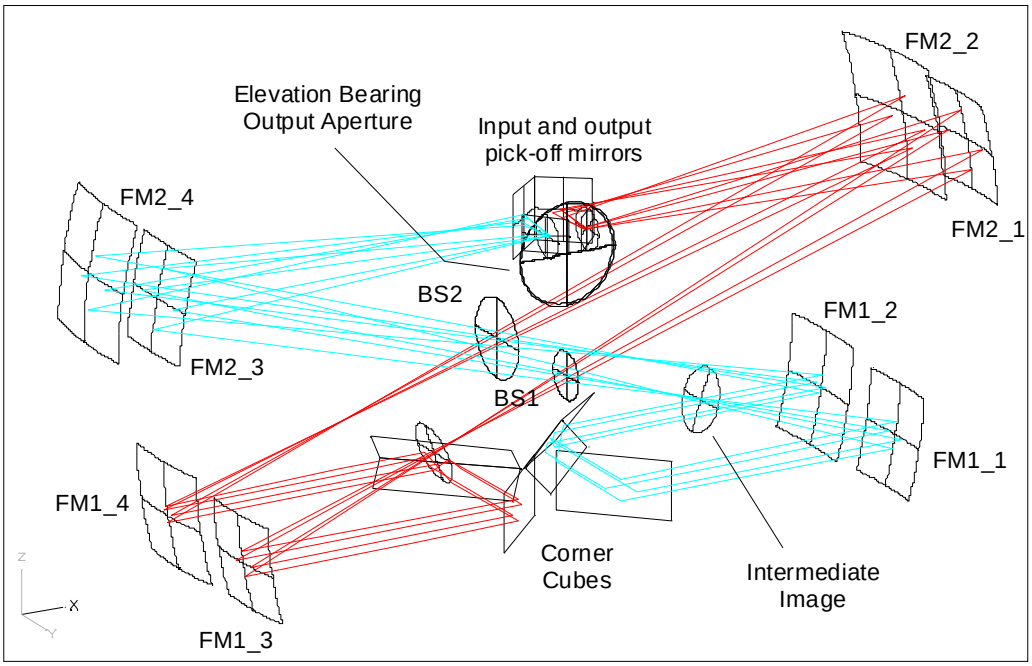

Figure 3. Folded optical layout of the FTS-2 system showing the sizes, locations and curvatures of the mirrors, as well as the intermediate image planes.

Since the two input ports are symmetrical about the telescope optical axis, the optical system is symmetrical for both ports; the mirrors for one port have the same curvature as the mirrors for the other port. The optical design can be represented more simply by the linear schematic for one port of the interferometer shown in Figure 4.

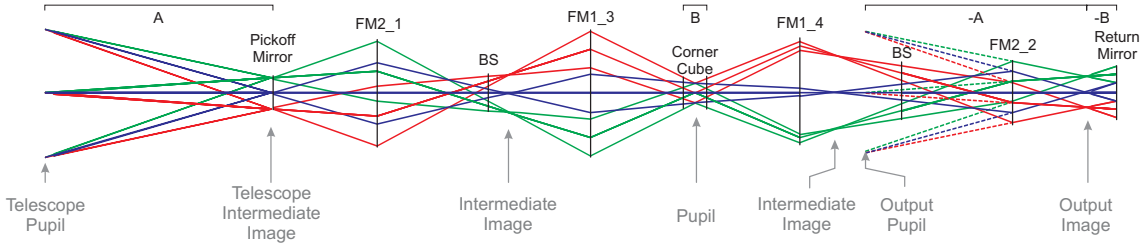

Figure 4. A simplified linear schematic for one port of the FTS-2 system, showing the approximate intermediate images and pupil locations. The telescope pupil and image are reproduced at the appropriate distances (-A nd –B) from the return pickoff mirror.

Aspherical powered mirrors are used within the FTS to constrain the expanding beam, in a design similar to the one first proposed by Dohlen[4]. For symmetry, a pupil is placed at the apex of the corner cubes when the moving mirrors are at zero path difference (ZPD). However, this pupil drifts as the mirrors translate during a scan (see Figure 5), and since the following mirrors are aspherical, there is spill-over on subsequent optics and misalignment of the image field points from both arms of the interferometer on the detector. The net effect is increased apodization in the interferograms due to vignetting and increased spot sizes at higher spectral resolution, and is more severe at the periphery of the field of view. At high resolutions, vignetting occurs primarily at the cold stop of

the detector, although there is also some vignetting within the second half of the interferometer and at the return mirrors.

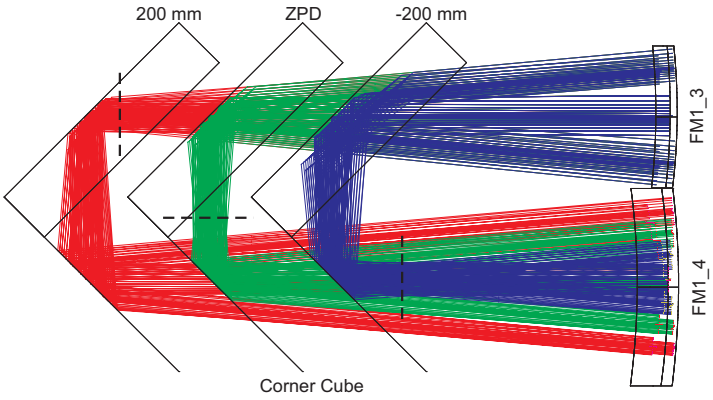

Figure 5. Pupil location (dotted lines) for one arm of the interferometer at corner cube positions of ZPD and +/- 200 mm relative to ZPD, as seen from above

Placing the return mirrors as close as possible to the pickoff mirrors reduces the required aperture for the return mirrors, and allows the lower two quadrants of the image to pass through unobstructed to the detector. Placing the return mirrors out of the plane of the output half of the interferometer, however, introduces a small image rotation relative to the non-FTS image, which must be corrected in software.

5. Optical Model

Optimization of the optical design was done using ZEMAX in collaboration with the Institut National d'Optique (INO) in Quebec, taking into account the design goals of maximizing the image quality, FOV, efficiency and spectral resolution within the constraints imposed by the available space envelope. The model was based on the final SCUBA-2/JCMT optical model, with the FTS optics inserted at the proper location. A full report of the model design and optimization results can be found in document INO 060140 R/09.

The model was optimized for 850 μm using the image field points shown in Figure 6.

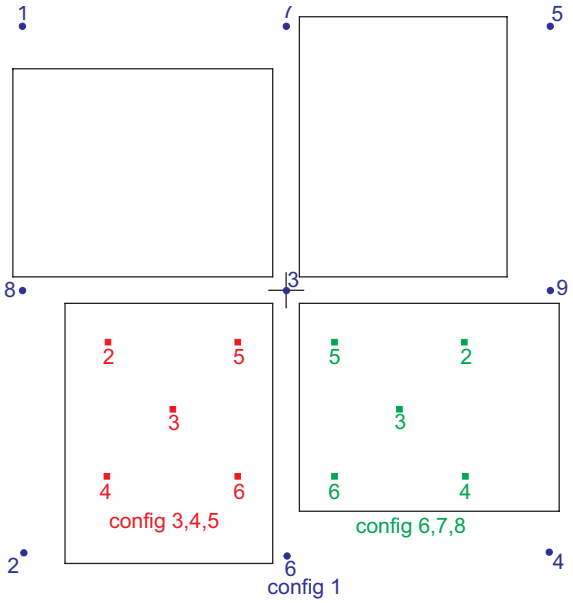

Figure 6. Field points used in the Zemax optical model. Configuration 1 (blue circles) represent the SCUBA-2 field points. The other configurations (red and green squares) represent the FTS-2 field points for both ports.

6. Performance

6.1. Image Distortions

The FTS output ports each represent the difference of the two input ports. As a result, the image on each subarray is identical (except that the interferograms are complimentary) but mirrored about the vertical axis. There is also a flip about the centre of the port relative to the non-FTS image, as shown below.

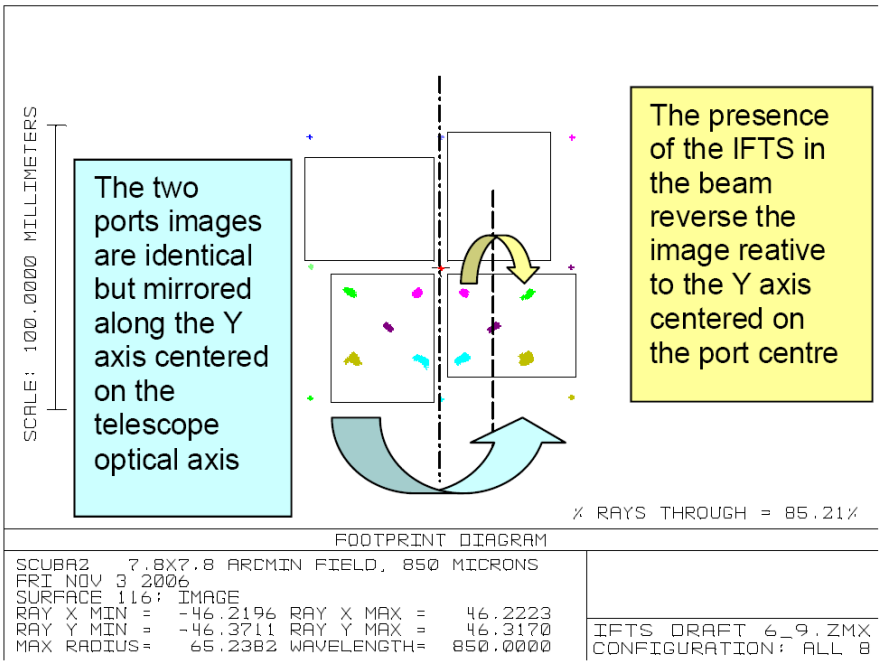

In addition to the basic mirroring, there is a slight rotation in each image about the port centre as a result of the output pickoff mirrors being slightly out of the plane of the second half of the interferometer.

At ZPD, the FTS image and the non-FTS image field points are coincident. Away from ZPD, there is an increasing magnification in the FTS image which results in a degradation of the interferogram contrast. See the INO report for a full analysis.

6.2. Vignetting

The maximum field of view of the FTS input ports is ultimately limited by the maximum practical mirror diameters (roughly 400 mm diameter) to approximately 5 arcmin^2. The computed fraction of rays passing through the FTS unvignetted and the interferogram contrast ratio (based on the relative vignetting between the two arms of the interferometer) for the central field point is given in Table 1 as a function of mirror travel distance from low to high spectral resolution. Table 2 shows the same data for a field point on the periphery of the FOV. The full analysis is in the INO report.

Table 1. Vignetting and contrast ratio for central field #3(-0.02876°, 0.02876°).

Travel distance	Side with increasing travel distance	Side with decreasing travel distance	Interference contrast, excluding image shift
ZPD	97.55%	97.55%	1.000
±15mm	98.01%	97.14%	0.991
±30mm	98.37%	96.89%	0.985
±50mm	98.83%	96.53%	0.977
±100mm	91.64%	94.44%	0.970
±150mm	91.64%	91.22%	0.995
±200mm	91.64%	91.69%	0.999

Table 2. Vignetting and contrast ratio for outer field #6 (-0.04543°, 0.04543°).

Travel distance	Side with increasing travel distance	Side with decreasing travel distance	Interference contrast, excluding image shift
ZPD	88.37%	88.37%	1.000
±15mm	92.20%	81.64%	0.885
±30mm	91.13%	74.40%	0.816
±50mm	82.56%	64.81%	0.785
±100mm	57.89%	42.02%	0.622
±150mm	36.41%	19.07%	0.524
±200mm	16.57%	2.19%	0.132

6.3. Spot Sizes

The spot size increases with travel distance and away from the centre of the FOV. The spots remain under the diffraction limit for travel distances between +200mm and –100mm, as shown below. See the INO report for full analysis.

Field #	2	3	4	5	6	
Travel (mm)	RMS spot radius (µm)					Airy Radius (µm)
200	1278.53	763.15	1519.94	2303.04	2574.04	2914
150	806.49	779.85	996.05	1051.42	1209.62	2870
100	778.35	798.99	1052.66	1214.97	1006.35	2827
50	562.32	822.46	930.40	836.87	1129.04	3788
30	624.24	830.38	911.04	627.23	1126.54	3673
15	780.40	835.56	1016.31	562.85	1061.97	3630
0	983.13	841.09	1252.08	610.48	1089.92	3591
-15	1015.77	846.36	1436.71	714.62	1136.45	3556
-30	968.78	853.11	1506.06	797.31	1197.13	3474
-50	903.07	853.28	1575.29	857.15	1305.42	3447
-100	2184.03	855.31	2864.79	1332.28	2219.53	3403
-150	5752.90	864.65	8149.83	3570.26	5222.30	3405
-200	1.10E+04	873.98	2.10E+04	7681.65	1.10E+04	3331

6.4. Beamsplitter

The performance of the MZ design depends critically on the beam splitter characteristics. The Cardiff University group has extended their expertise in manufacturing metal mesh resonant filters to the production of a new type of intensity beamsplitters with 4RT efficiencies above 90% and a factor of 4 in frequency range, as shown in Figure 7. This beamsplitter uses two metal meshes in a Fabry-Perot configuration designed to meet the 50% transmission and 50% reflection criteria of an ideal intensity beamsplitter. One serendipitous feature of these beamsplitters is that they also function sufficiently well at optical wavelengths that a laser can be used to check the alignment of the interferometer.

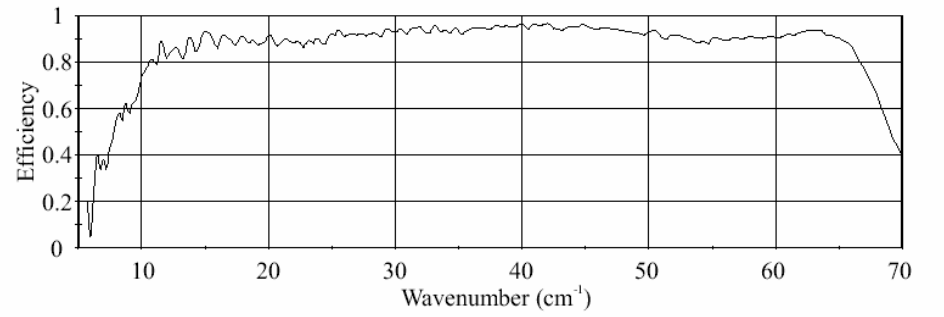

Figure 7. Measured beamsplitter efficiency.

One concern with the new beamsplitters was the possibility of a non-linear, port dependent phase. This is, of course, of significant importance to the SPIRE mission

where the second input port will be used to null the emission from the warm Herschel telescope. Our group is responsible for the SPIRE data analysis software and recent analysis of the SPIRE flight model spectrometer data (Figure 8) has shown that this phase is well behaved.

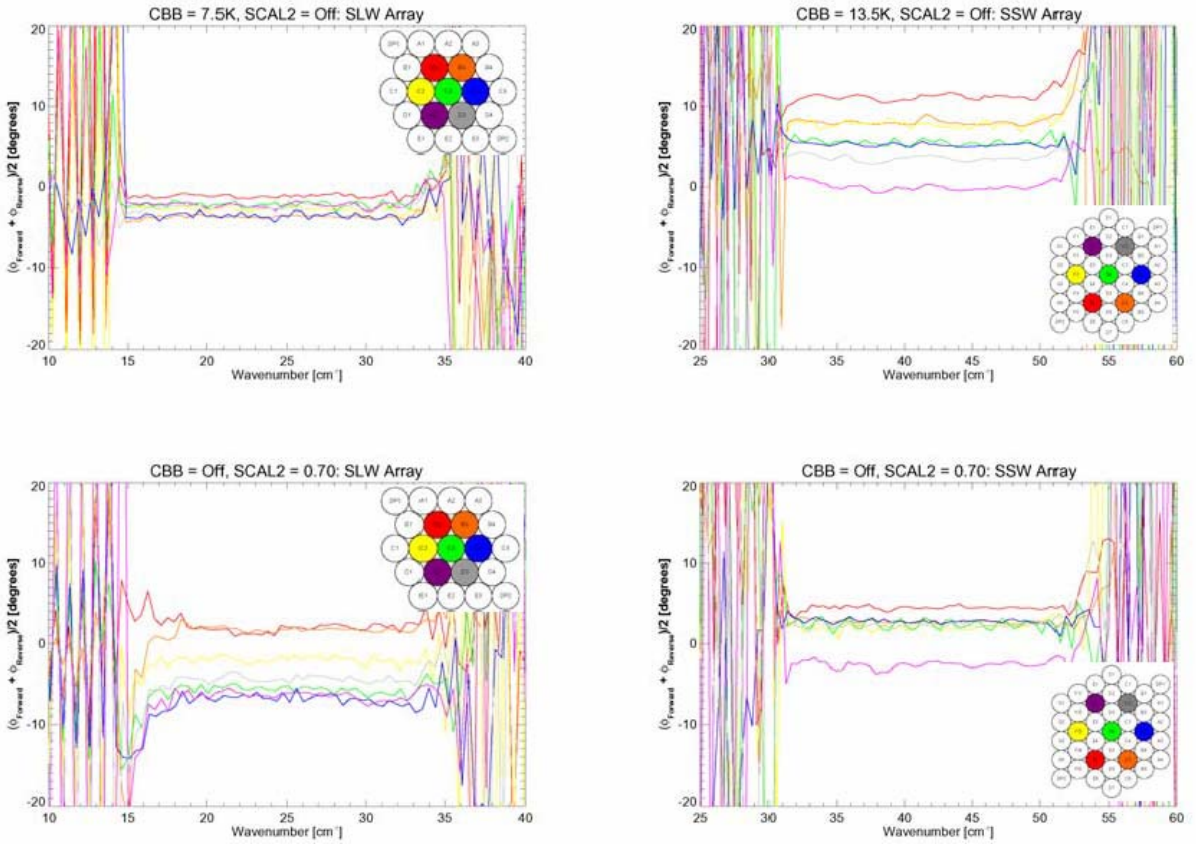

Figure 8. Optical Phase determined with the SPIRE MZ FTS. Top Left: Cold Blackbody (CBB) input, Long Wavelength (SLW) Array; Top Right: CBB input, Short Wavelength (SSW) Array; Bottom Left: Spectrometer Calibration source (SCAL) input, SLW Array; Bottom Right: SCAL input, SSW Array.

As can be seen from the plots in Figure 8, the derived optical phase is well behaved over each optical passband. Furthermore, inter-pixel differences in the offset of the optical phase are consistent between scans, as in the case of the electrical phase.

7. Tolerancing

Monte Carlo tolerancing analysis was performed by INO. For all FTS optics, the allowed decentre in XYZ is 200 μm and the allowed tilt misalignment is 0.5°. These tolerances are easily met by conventional machining techniques and the adjustability of the FTS-2 optical mounts. The full tolerancing report is not available at the time of writing.

8. Mirror Prescriptions

The full mirror prescription report is contained in document SC2/FTS/OPT/004.

References

[1] Ade, P.A.R, Hamilton, P.A., and Naylor, D.A. An Absolute Dual Beam Emission Spectrometer. *Optical Society of America*, FTS topical meeting poster FWE3, Santa Barbara, California, June 1999.
[2] Naylor, D.A., Gom, B.G., Schofield, I.S., Tompkins, G.J., Davis, G.R. Mach-Zehnder Fourier transform spectrometer for astronomical spectrocopy at submillimeter wavelengths. *Proc. SPIE, Millimeter and Submillimeter Detectors for Astronomy* **4855**, 540-551 (2003).
[3] Swinyard, B.M., Ade, P.A.R, Griffin, M.J., Dohlen, K., Baluteau, J., Pouliquen, D., Ferand, D., Dargent, P., Michel, G., Martignac, J., Rodriguez, L., Jennings, D., Caldwell, M., Richards, A., Hamilton, P., and Naylor, D.A. The FIRST-SPIRE Spectrometer: A Novel Imaging FTS for the Sub-Millimetre. *Proc. SPIE, UV, Optical, and IR Space Telescopes and Instruments* **4013**, 196-207 (2000).
[4] B.M. Swinyard, K. Dohlen, D. Ferand, J. –P. Baluteau, D. Pouliquen, P. Dargent, G. Michel, J. Martignac, P. Ade, P. Hargrave, M. Griffin, D. Jennings, and M. Caldwell, "The Imaging FTS for Herschel SPIRE", *Proc. SPIE: IR Space Telescopes and Instruments* **4850**, pp. 698-709, (2003)